Multiresolution Analysis and Classification of Textured SAR Image

Liu Guoqing Huang Shunji
(Dept. of Electronic Engineering, UEST of China Chengdu 610054)

Abstract This paper studies the multiresolution analysis and classification of the textured synthetic aperture radar (SAR) image using the wavelet transform (WT). The tree-structured WT algorithm is first employed to decompose a real-world textured SAR image, and to quantify different texture types in the image. Then, the pyramid-structured WT algorithm is applied in multiresolution classification of the image. The classification result obtained demonstrates the advantage of the WT in the textured SAR image classification.

Key words synthetic aperture radar; wavelet transform; multiresolution analysis; texture

In general, the speckle-reduced synthetic aperture radar (SAR) image consists of textures of natural terrain and artificial objects. It is therefore called the textured SAR image. Due to natural fluctuations of the scene, the textures in SAR images appear as nonstationary signals, and are difficult to quantify with a conventional transform (*e.g.* Fourier transform).

During the last decade, the wavelet transform (WT) has been of great interest of the analysis of nonstationary signals. With the WT, a nonstationary signal can be transformed into a representation which is localized in both time and frequency domains simultaneously[1~3]. The detailed information of the nonstationary signal can be also extracted by the wavelet multiresolution decomposition[1]. Recently, the application of the WT in image segmentation has received wide attention due to its such ability of extracting the multiresolution information.

1 WT Multiresolution Decomposition

The wavelet transform results in a decomposition of a signal with a family of orthonormal bases obtained through the translation and dilation of the wavelets[1]. Using the WT to decompose a one-dimensional signal into lower resolution levels demands a scaling function $\varphi(x)$ and a wavelet $\psi(x)$[1]. In an $(L+1)$-level wavelet decomposition, letting $A_0 f(n)$, $A_1 f(n)$, …, $A_L f(n)$ be the discrete representations of the original signal $f(x)$ at resolution levels 0, 1, …, L, with $A_0 f(n) = f(n)$, the difference between $A_l f(n)$ and $A_{l+1} f(n)$ be the detail signal at resolution level l denoted by $D_l f(n)$, the wavelet multiresolution decomposition of the discrete signal $f(n)$ has been shown to be a recursive filtering porcedure starting from $f(n)$ with a pair of quadrature mirror filters[1]

$$A_l f(n) = \sum_k h(k-2n) A_{l-1} f(n) \tag{1}$$

$$D_l f(n) = \sum_k g(k-2n) A_{l-1} f(n) \tag{2}$$

Received October 30, 1996 and revised September 30, 1997

where $h(n)$ and $g(n)$ are low and high pass filters, respectively, and their coefficients are related to $\varphi(x)$. Choosing the resolution step to be 2, the filtered results are subsampled by a factor 2. This decomposition is performed recursively to the outpet of $h(n)$, and is thus called the pyramid-structured wavelet decomposition.

The two-dimensional wavelet decomposition can be implemented with the following four filters

$$\begin{aligned} A(n_x, n_y) &= h(n_x)h(n_y) \qquad B(n_x, n_y) = g(n_x)h(n_y) \\ C(n_x, n_y) &= h(n_x)g(n_y) \qquad D(n_x, n_y) = g(n_x)g(n_y) \end{aligned} \tag{3}$$

where, for instance, filter $C(n_x, n_y) = h(n_x)g(n_y)$ means the filters $h(n)$ and $g(n)$ are used sequentially for filtering in the x and y directions, n_x and n_y are sampling sequences in the x and y directions, respectively.

The conception of wavelet bases has been generalized to include a library of modulated waveform orthonormal bases called wavelet packets[3]. This generalization leads to a new type WT called the tree-structured WT. The key difference between this idea and the pyramid-structured WT is that the decomposition is no longer simply applied in the low frequency channel recursively. Instead, it can be applied in the output of any filter A, B, C, or D in Eq. (3). In practice, it is unnecessary and expensive to decompose all subimages obtained in each resolution level to achieve a full decomposition. A convenient approach to avoid a full decomposition, is to evaluate the energy functions of the subimages in the same resolution level. If the energy of a subimage is significantly smaller than those of others, this subimage will not be dealt with in the next decomposition step.

2 Multiresolution Texture Analysis

The highest resolution speckle-reduced image (shown in Fig. 1) to be analyzed consists of (800×1 024) pixels with (10 m×10 m) spatial resolution. This image is obtained by applying the multi-look polarimetric whitening filter (MPWF)[4] in the 4-look polarimetric SAR data acquired by the NASA/JPL airborne L-band polarimetric SAR over the San Franciso Bay area.

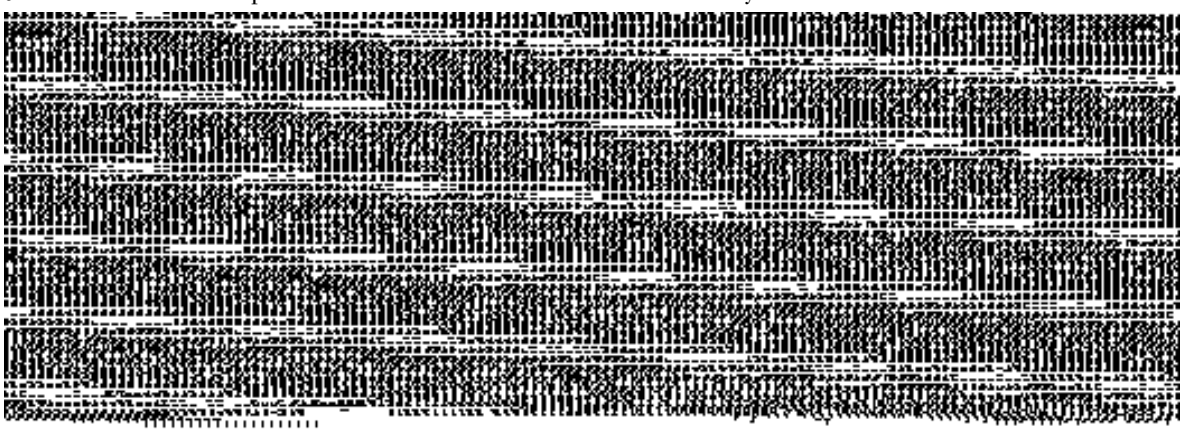

Fig. 1 Original textured SAR image

Fig. 2 Tree-structured wavelet decomposition

Three resolution levels are generated for texture analysis. Fig. 2 exhibits the results of using the tree-structured wavelet decomposition. Recorded in Table 1 are the average energy functions of the de-

composed images. The symbol "A" in Tabe 1, for example, means that the image "A" is the output of filter A in Eq. (3), and "AB" refers to the output of filter B when acting on the image A. The average energy, E, of an image is defined as

$$E = \frac{1}{M_a M_r} \sum_{i=1}^{M_r} \sum_{j=1}^{M_a} I_{ij} \tag{4}$$

where M_a and M_r are the numbers of azimuth and range lines, respectively, and I_{ij} represents the intensity value of the pixel located in the i-th range line and the j-th azimuth line. The image D in the first resolution level is not further decomposed since it has poor energy compared with other subimages in the same level, its average energy is less than 15% of image A which has the largest average energy in this level. Results in Tabel 1 show obviously that significant information of this textured image is concentrated in lower frequency channels.

Table 1　Average energy function

resolution level		image and average energy											
0	$\bar{E}$	160.5											
1	image	A				B				C			D
	$\bar{E}$	160.7				33.8				40.6			22.3
2	image	AA	AB	AC	AD	BA	BB	BC	BD	CA	CB	CC	CD
	$\bar{E}$	162.3	47.2	40.2	28.1	34.3	11.8	13.4	9.2	41.2	17.3	15.7	13.4

Using principal images in each resolution level, we now present a quantitative comparison between different texture types. Tabel 2 shows the average energy for each texture type in each level. Among three types of texture, the city texture covers widest spectral range, four subbands can be found in the second resolution level whose energy functions are greater than 25% of that of the largest energy subband. The ocean surface is almost completely governed by texture contents in the lowest spectral range. The spectral distribution of the forest-like texure is somewhat similar to that of the city-like texture but with only one subband whose energy is greater than 20% of that of the largest energy subband. These analyses imply that the texture in the city area has strong variation, and the ocean surface has little fluctuation relative to the other two types of texture.

Consequently, we know the principal contents of all three texture types are concentrated in low frequency channels. This suggests, for this image, the pyramid-structured wavelet decomposition could alone provide adequate information for the multiresolution image classification.

Table 2　average energy of texture

resolution level		ocean					forest-like					city				
0	$\bar{E}$	44.8					89.5					394.6				
1	image	A			B	C	A			B	C	A			B	C
	$\bar{E}$	44.9			4.6	7.2	89.7			12.0	17.6	393.4			94.9	103.0
2	image	AA	AB	AC	BA	CA	AA	AB	AC	BA	CA	AA	AB	AC	BA	CA
	$\bar{E}$	44.9	4.3	4.3	4.5	7.2	90.1	19.0	13.5	12.0	17.5	387.5	117.0	109.6	93.1	101.7

3　Multiresolution Image Classification

Applying the WT in the image classification implies to implicitly utilize the spatial contextual in-

formation because each pixel in a lower resolution level represents an optimal block of pixels in a higher resolution level. When the classification results obtained in a lower resolution level are used for guiding a higher resolution classification, the robustness of the classification algorithm can thus be guaranteed.

To classify this textured SAR image (named as classification 1) without supervision, we first estimate the proper number of texture classes and their model parameters in the lowest resolution level using the unsupervised classification algorithm presented in Ref. [5], and then classify the image progressively from the lowest to the highest resolution level until individual pixels are well classified. The unsupervised classification in the top of the pyramid verifies that there are six texture classes existing in the image. For comparison, this image is also classified without applying the WT (named as classification 2).

Concerning the computational requirement, the average number of visits per pixel is reduced by more than one-half in the classification 1 with respect to that in the classification 2. This means the computational efficiency is improved over 50% by using the WT. For evaluating the classification performance, we evaluate the correspondence between the classification result and the actual textures in the image. This test, of course, requires supervised knowledge of the image. In practice, six subareas are selected for each texture class, and percentages that pixels within each subarea belong to each class are computed to evaluate the probabilities of correct classification. Table 3 lists such estimated results. The quantitaitve comparison distinctly demonstrates that the classification based on the multiresolution analysis outperforms that without the multiresolution scheme.

Tabel 3 Probability of correct classification

classification	ocean 1	ocean 2	park	city 1	city 2	city 3	total
classification 1	99.9	98.3	69.3	40.8	52.1	47.3	70.0
classification 2	99.9	99.4	65.5	19.9	21.7	18.1	54.1

4 Conclusions

We have investigated the multiresolution analysis and classification of the textured SAR image with the WT. The multiresolution SAR image classification experiment with the pyramid-structured WT demonstrated the advantage of the WT in both speeding up the classification procedure and improving the classification performance. In addition, we remark that the tree-structured WT algorithm has provided a powerful tool for multiresolution texture analysis and classification for images in which the principal contents may be distributed in different frequency channels other than the lowest frequency channel.

参 考 文 献

1 Mallat S G. A theory for multiresolution signal decomposition: the wavelet representation. IEEE Trans on PAMI, 1989, 11(7): 674~693

2 Daubechies I. The wavelet transform, time-frequency location and signal analysis. IEEE Trans on IT, 1990, 36(5): 961~1 005

3 Coifman R R, Wicherhause M V. Entropy-based algorithms for best basis selection. IEEE Trans on IT,

1992, 38:713～718

4 Liu Guoqing, Huang Shunji, Tore A et al. Optimal speckle reduction in multilook polarimetric SAR image. Proc of 1995 International Geoscience and Remote Sensing Symposium－IGARSS′95, 1995:664～666

5 Liu Guoqing. Theoretical analysis and applications of polarimetric SAR imaging. Doctoral dissertation, Univ of Electr Sci and Tech of China, Chengdu, 1996:93～126

纹理 SAR 图像的多分辨率分析和分类

刘国庆*　　黄顺吉

（电子科技大学电子工程系　成都　610054）

【摘要】 应用小波变换研究纹理合成孔径雷达(SAR)图像的多分辨率分析和分类，首先应用树状结构的小波变换算法对一幅纹理SAR 图像进行多分辨率分解，并对图像中的不同纹理类型进行定量分析，然后将金字塔结构的小波变换算法应用到图像的多分辨率分类，所得结果证明了小波变换在纹理SAR 图像分类中的优越性。

关　键　词　合成孔径雷达；　小波变换；　多分辨率分析；　纹理；

中图分类号　TN 957.52；　TN 957.524

编辑　叶　红

·科研成果介绍·

程控调谐微波滤波器系列

主研人员：黄尚锐　王晓军　姚　毅　刘承功　丁文洪　唐　璞

程控调谐微波滤波器为机械调谐微波滤波器，经电机带动，同步调谐，研制出可达倍频程调谐的调谐方法，调谐范围达到 46.6%；成功地解决了在 46.6% 的调谐范围内带宽变化小于 20%，远小于法国 TFH701 中同类型滤波器的带宽变化率的实测指标(84.6%)，在整个调谐范围内特性基本保持一致；解决了用空心杯电机调谐带来的功率小及过冲问题；腔体用 8 块板拼装而成，同时解决了泄漏问题。

该滤波器系列性能良好，经对比测试达到或超过国外同频段同用途的滤波器指标。

信号细微特征提取分析技术

主研人员：肖先赐　魏　平　陆明泉　毛国安　朱晓霞　邹月娴 等

信号微特征提取分析技术包括雷达信号中频数字录取实验模型、雷达信号细微特征分析，通信信号中频数字录取实验模型、通信信号细微特征分析和电子战信号分析软件五个方面的内容。研究了一种基于 AR 模型参数估计的模式识别方法来识别雷达个体特征。提出了通信信号细微特征选取的准则，在功率谱、谱相关、高阶谱域中提取通信信号特征，并用神经网络方法进行信号识别。

该项成果在通信信号识别方法方面具有创新性，其在信号识别方面具有广泛应用前景。

·科　卞·

1996 年 10 月 30 日收稿，1997 年 9 月 30 日修改定稿

* 男　32 岁　博士　副教授